DOI: 10.1002/ejic.200700503

Proton NMR Study of Low-Spin *meso*-Unsubstituted β-Substituted Alkyl Iron Porphyrins: Remarkable Influence of Peripheral Substitution on Spin Density

Sandrine Juillard,[a] Arnaud Bondon,[b] and Gérard Simonneaux*[a]

Keywords: NMR spectroscopy / Porphyrinoids / Iron / HMBC / Saturation transfer

Paramagnetic NMR spectroscopy was used to characterize the influence of small alkyl groups on the spin density of a series of high-spin and low-spin iron(III) porphyrins. Assignment of the resonances was obtained by using a variety of NMR techniques including heteronuclear multiple bond correlation and saturation transfer experiments.

Introduction

Heme is one of the most versatile prosthetic groups in metalloproteins, and different types of heme have been found in proteins.[1] The reconstitution of heme proteins with modified heme is a useful method for understanding the physiological function and creating a new function in heme proteins.[2] Many heme modifications with different substituents have been designed to optimize heme/apoprotein interaction and even an iron porphine complex has been employed as the smallest prosthetic group of heme protein to modify intensively the heme–globin interactions.[3] Recently, we prepared myoglobin (rMb) reconstituted with the iron complex of 3,7-diethyl-2,8-dimethylporphyrin[4] in which two ethyl groups were found to be large enough to avoid the free rotation movement of the heme.[5] However, to discuss the contribution of individual pyrroles in myoglobin, it is quite interesting to design smaller porphyrins such as 3-ethyl-2-methylporphyrin. In this study, we used paramagnetic NMR spectroscopy to characterize the influence of small alkyl groups on the spin density of a series of high-spin and low-spin iron(III) porphyrins, including low-spin bis(cyanido)-3-ethyl-2-methylporphyriniron(III).

Results and Discussion

The synthesis of β-pyrrole-substituted porphyrins has been reported elsewhere,[4] and iron was inserted to produce $Fe^{III}Cl$ porphyrins as outlined in the Experimental Section. The UV/Vis spectra of these complexes are compatible with high-spin, five coordinate structures. The structures of the compounds are summarized in Figures 1 and 2.

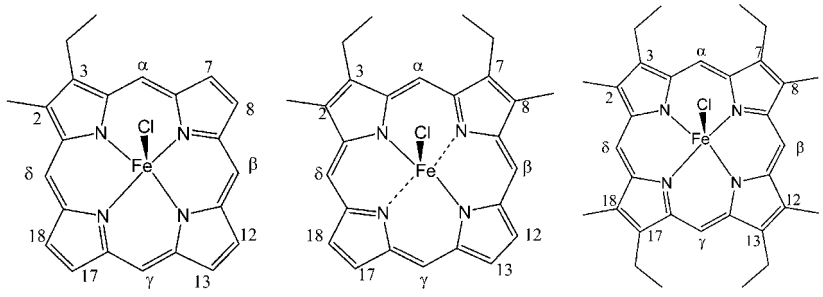

1·$Fe^{III}Cl$ **2**·$Fe^{III}Cl$ **3**·$Fe^{III}Cl$

Figure 1. The structures of β-pyrrole-substituted FeCl porphyrin complexes.

[a] Laboratoire de Chimie Organométallique et Biologique, UMR CNRS 6226 Campus de Beaulieu,Université de Rennes 1, 35042 Rennes, France
[b] RMN-ILP, UMR CNRS 6026, IFR 140 PRISM, Campus de Villejean, Université de Rennes 1, 35043 Rennes, France

High-Spin Complexes

The ^1H NMR spectrum of **1**·FeCl in [D_1]chloroform at 298 K is shown in Figure 3a. The relative intensities of the peaks and their comparison with ^1H NMR spectroscopic

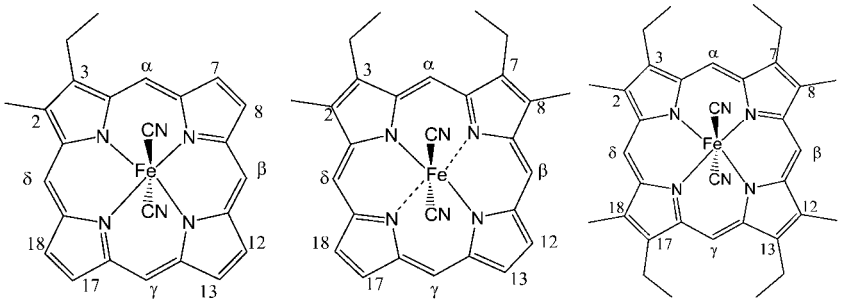

Figure 2. The structures of β-pyrrole-substituted $Fe(CN)_2$ porphyrin cmplexes.

results previously reported for octaethylporphyriniron chloride[6–8] determined their assignment. Two resonances for the *meso* protons are observed in the highfield region at δ = –63.3 and –58.3 ppm. In the downfield part of the spectrum, three resonances are found at $\delta \approx 78$ ppm for the β-pyrrole protons as a result of accidental overlap, as the absence of symmetry dictates that there should be six β-pyrrole resonances. Also in the downfield part of the spectrum, one resonance at δ = 51.3 ppm for 2-CH_3 and two resonances at δ = 39.9 and 43.7 ppm for the ethyl group of 3-CH_2CH_3 appear owing to diastereoisomerism. The CH_3 resonance of the ethyl group is not assigned because of its presence under the diamagnetic area. The ^{1}H NMR spectra of the other complexes of this type **2**·FeCl and **3**·FeCl have related features, although the presence of idealized C_s symmetry greatly simplifies the spectrum. Thus, **2**·FeCl has three *meso* protons with a 1:2:1 intensity ratio in the upfield region, two resonances at δ = 76.8 and 79.1 ppm for the β-pyrrole protons as a result of accidental overlap, two resonances at δ = 40.4 and 43.3 ppm for the 3,7-CH_2CH_3 group owing to diastereoisomerism, and a resonance at δ = 54 ppm for the 2,8-CH_3 group. As expected for **3**·FeCl, only two broad resonances are observed at δ = –54.9 and –56.6 ppm for the *meso* protons. The chemical shifts for the three complexes are summarized in Table 1 (298 K), and all of them are compatible with a high-spin state, S = 5/2.[9]

Table 1. ^{1}H NMR chemical shifts [ppm] of high-spin iron porphyrin chloride in $CDCl_3$ (298 K).

Complex	*meso*-H	CH_2CH_3	CH_2CH_3	β-pyrrole-H
1·$Fe^{III}Cl$	–58.3	39.9	51.3	76.8
	–63.3	43.7		77.7
				78.6
2·$Fe^{III}Cl$	–53.8	40.4	54.0	76.8
	–59.3	43.3		79.1
	–63.3			
3·$Fe^{III}Cl$	–54.9	40.5	52.5	–
	–56.6	43.9		
$TPPFe^{III}Cl$[a]	–	–	–	–72.4
$OEPFe^{III}Cl$[b]	–55.5	41.6	–	–
		43.7		

[a] At 293 K, TPP: tetraphenylporphyrin.[33] [b] At 298 K, OEP: octaethylporphyrin.[8]

The typical spin delocalization pathways for high-spin iron(III) porphyrins produce resonances for the β-pyrrole and α-CH_2 protons that are strongly shifted downfield.[10] Accordingly, all the iron(III) chloride complexes **1**·FeCl, **2**·FeCl, and **3**·FeCl showed this behavior. This downfield shift is mainly a result of the σ-contact contribution that results from delocalization through the σ-framework by way of σ-donation to the half-occupied $d_{x^2-y^2}$ iron(III) orbital. Comparison of the ^{1}H NMR spectroscopic data of the high-spin, five coordinate iron(III) complexes shown in Table 1 also shows that substitution produces a small effect on the chemical shift of the *meso* resonances with electron-donating groups (alkyl groups), shifting these resonances in a downfield fashion. The β-pyrrole protons are found to resonate in a narrow window from δ = 76 to 79 ppm.

Low-Spin Complexes

The addition of an excess amount of potassium cyanide to the iron chloride complexes in the NMR tube gave the low-spin bis(cyanido)iron complexes (see Experimental Section). Thus the ^{1}H NMR spectrum of K[**1**·$Fe(CN)_2$] in methanol/chloroform at 308 K (Figure 3b) shows six resonances for the β-pyrrole protons in the high-field region, as expected from the absence of symmetry in the structure. Because HMBC spectra were not informative in this particular case, assignments of these protons were obtained by means of 1D NOE difference spectroscopy as well as 2D COSY spectroscopy. For example, all required cross peaks were identified in the COSY spectrum (Figure 4), allowing notably the identification of each pair of the β-pyrrole protons. The NOE difference spectrum, recorded at 308 K (Figure 5a), outlines the increase in intensity for the *meso* proton α-H at δ = 2.93 ppm and the β-pyrrole proton 7-H at δ = –11.75 ppm when the ethyl group at δ = 8.51 ppm was irradiated. Following the COSY spectrum, this situation identifies the proton 8-H at δ = –14.75 ppm. To complete the assignment, the NOE difference spectrum showed an increase in the intensity for the *meso* proton δ-H at δ = 2.56 ppm and the β-pyrrole proton 18-H at δ = –11.89 ppm when the methyl group (2-CH_3) at δ = 18.46 ppm was irradiated (Figure 5b). The signal at δ = –14.37 ppm was as-

signed to 17-H, whereas the last two *meso* protons at δ = 0.32 and 0.38 ppm were assigned to β-H and γ-H without a respective assignment. The last two β-pyrrole protons at δ = –12.96 and –13.05 ppm were assigned to 12-H and 13-H without a respective assignment. The chemical shift values obtained at 298 and 308 K for K[**1**·Fe(CN)$_2$] are summarized in Table 2. They are all compatible with a low-spin state, S = 1/2.

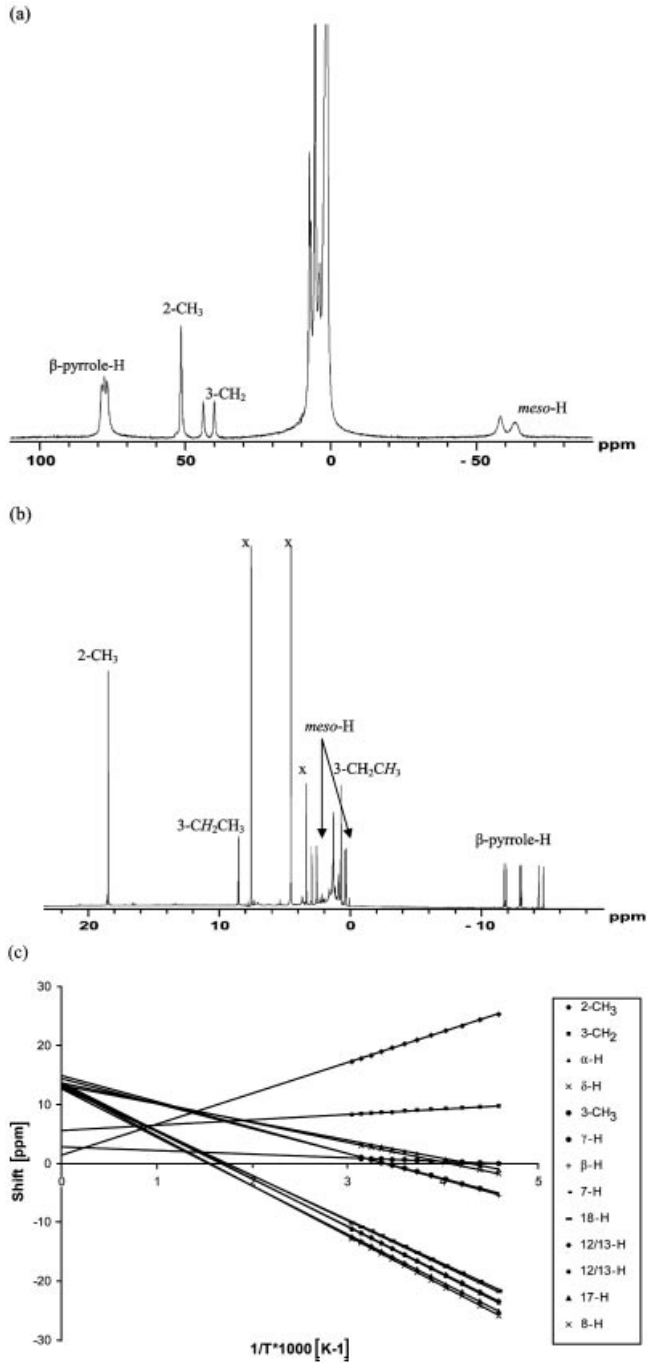

Figure 3. ^{1}H NMR spectrum for (a) **1**·Fe^{III}Cl in $CDCl_3$ at 298 K, (b) K[**1**·Fe(CN)$_2$] in $CDCl_3$/MeOD (60:40) at 308 K, x: solvent peaks, and (c) Curie plots for K[**1**·Fe(CN)$_2$].

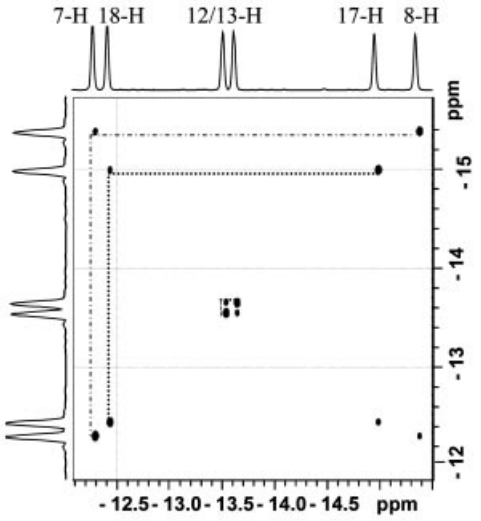

Figure 4. Part of the COSY spectrum showing β-pyrrole protons for K[**1**·Fe(CN)$_2$] (298 K).

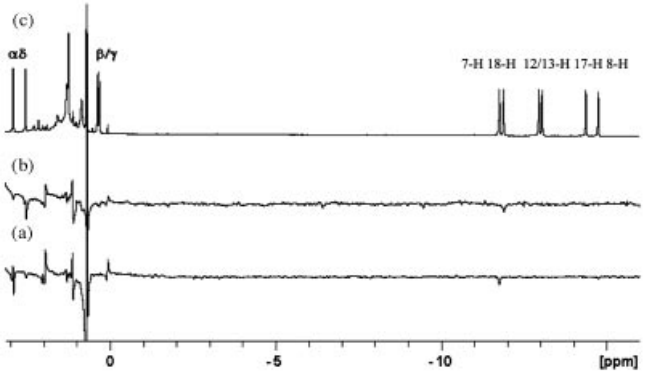

Figure 5. 1D NOE difference spectra for K[**1**·Fe(CN)$_2$] at 308 K: (a) irradiation of the CH_2 group at δ = 8.51 ppm, (b) irradiation of the CH_3 group at δ = 18.46 ppm, (c) high-field part of the spectrum.

The ^{1}H NMR spectrum of K[**2**·Fe(CN)$_2$] in methanol/chloroform at 298 K (Figure 6a) shows two resonances for the β-pyrrole protons in the highfield region, as expected from the symmetry of the structure. A complete assignment of all the protons was obtained by means of heteronuclear correlation spectroscopy (HMQC and HMBC) as well as 2D COSY spectroscopy. The relative intensities of the resonances and the COSY spectrum allowed the assignment of all the protons except for the two *meso* protons, α and γ, and the β-pyrrole protons. It was previously reported that HMQC spectroscopy of paramagnetic iron porphyrins provides the scalar heterocorrelation under natural abundance conditions of ^{13}C.[11] In the present study, this correlation technique offers a route to identify the β-pyrrole resonances by taking advantage of the fact that the full assignment of the proton signals of the β-^{13}C-^{1}H pairs has been established. Thus, the signal assignment of the carbons with directly bonded protons such as β-pyrrole protons and *meso* protons (^{13}C-^{1}H) was done on the basis of HMQC experiments. The assignment was then completed with the

Table 2. ^{1}H chemical shifts [ppm] of low-spin bis(cyanido)iron porphyrins in $CDCl_3/CD_3OD$ (60:40) (298 K).

Complex	β-pyrrole-H	*meso*-H	CH_3	CH_2CH_3	CH_2CH_3
K[**1**·Fe(CN)$_2$]	–15.32 (–14.75)[d]	0.07 (0.32)	18.89	8.62	0.68
	–14.93 (–14.37)	0.12 (0.38)	(18.46)	(8.51)	(0.71)
	–13.59 (–13.05)	2.38 (2.56)			
	–13.49 (–12.96)	2.77 (2.93)			
	–12.38 (–11.89)				
	–12.25 (–11.75)				
K[**2**·Fe(CN)$_2$]	–14.49	–0.66	18.87	7.02	0.50
	–11.73	1.29			
		3.72			
K[**3**·Fe(CN)$_2$]	–	1.43	16.71	7.30	0.44
		2.18			
K[Fe(OEP)CN$_2$][a]	–	3.32	–	7.35	
K[Fe(TPP)CN$_2$][b]	–11.68				
K[Fe(Porphine)CN$_2$][c]	–13.8	1.8			

[a] OEP: octaethylporphyrin in CD_3OD.[8] [b] TPP: tetraphenylporphyrin in CD_2Cl_2/CD_3OD at 202 K.[21] [c] At 298 K.[23] [d] At 308 K.

HMBC spectrum (Figure 7). For example, the ^{13}C signal at δ = 76.18 ppm (a β-pyrrole carbon) that showed correlation peaks with the proton signal at +1.29 ppm (*meso* β,δ-H) was assigned to C-12 and C-18. Consequently, the proton resonance at δ = –11.48 ppm was assigned to the β-pyrrole protons 12,18-H by using the HMQC spectrum. Similarly, the signals at δ = –14.49, –0.66, and 3.72 ppm were assigned to the identical β-pyrrole protons, 13-H and 17-H, and the *meso* protons, γ-H and α-H, respectively.

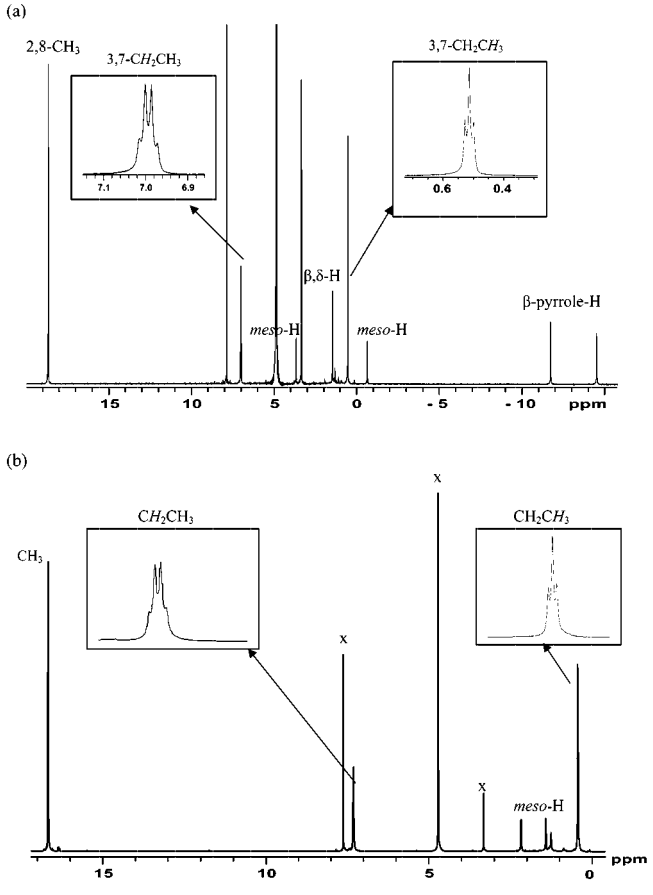

Figure 6. ^{1}H NMR spectra at 298 K for (a) K[**2**·Fe(CN)$_2$] and (b) K[**3**·Fe(CN)$_2$] in $CDCl_3$/MeOD (60:40).

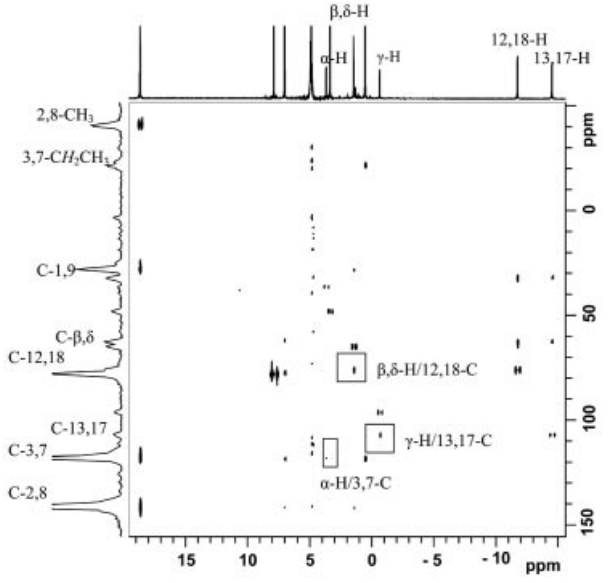

Figure 7. HMBC spectrum for K[**2**·Fe(CN)$_2$] at 298 K in $CDCl_3$/MeOD (60:40).

The ^{1}H NMR spectrum of K[**3**·Fe(CN)$_2$] in methanol/chloroform at 298 K is shown in Figure 6b. As previously described for K[**2**·Fe(CN)$_2$], complete assignment of the protons and carbons was obtained by means of HMQC and HMBC spectroscopy as well as 2D COSY spectroscopy (not shown). Comparison of the *meso* proton and *meso* carbon chemical shifts of K[**3**·Fe(CN)$_2$] with K[**1**·Fe(CN)$_2$] and K[**2**·Fe(CN)$_2$] reveals that the former complex also shows mainly a $(d_{xy})^2(d_{xz},d_{yz})^3$ electronic ground state. The proton chemical shifts for K[**2**·Fe(CN)$_2$] and K[**3**·Fe(CN)$_2$] are also summarized in Table 2; all are compatible with a low-spin state, S = 1/2.

Analysis of the curve in the Curie plot was made for K[**1**·Fe(CN)$_2$], K[**2**·Fe(CN)$_2$], and K[**3**·Fe(CN)$_2$]. As an example, the temperature dependences of the chemical shifts of the protons of K[**1**·Fe(CN)$_2$] in MeOD/$CDCl_3$ are shown in Figure 3c. The chemical shifts vary linearly with 1/T, but the extrapolated lines do not pass through the diamagnetic

value at $1/T = 0$. However, the intercepts at $1/T = 0$ for these signals were located between 0 and 15 ppm, and the chemical shift differences, if we consider the free-base porphyrin as a reference, do not vary to a great extent (less than 5 ppm). Similar results were obtained for the Curie plots of K[**2**·Fe(CN)$_2$] and K[**3**·Fe(CN)$_2$].

^{13}C NMR chemical shifts can also be a good probe to determine the electronic ground state, because they give the information on the spin distribution of any porphyrin carbons including *meso* and β-pyrrole carbons.[12,13] Table 3 shows the ^{13}C NMR chemical shifts for K[**1**·Fe(CN)$_2$], K[**2**·Fe(CN)$_2$], and K[**3**·Fe(CN)$_2$] at 298 K. Signals were obtained and assigned on the basis of HMQC spectra. Examination of the data in Table 3 reveals that the *meso* carbons appear in a range of 35–97 ppm, and the β-pyrrole carbons appear in a range of 70–142 ppm.

Table 3. ^{13}C chemical shifts [ppm] of low-spin bis(cyanido)iron porphyrins in $CDCl_3/CD_3OD$ (60:40) (298 K).

Complex	β-pyrrole-C	*meso*-C	CH_3	CH_2CH_3	CH_2CH_3
K[**1**·Fe(CN)$_2$]	72.1	51.4	–39.9	–27.1	86.9
	74.1	53.8			
	94.6	83.1			
	94.8	83.3			
	102.0				
	104.0				
K[**2**·Fe(CN)$_2$]	76.18	35.8	–42.2	–22.7	77.8
	107.5	65.4			
	107.7	97.3			
	142.1				
K[**3**·Fe(CN)$_2$]	127.4	57.1	–37.46	–22.5	77.7
	131.8	60.3			

Electronic Ground State of Low-Spin Complexes

The spin density distribution at the pyrrole positions in low-spin iron(III) complexes of disymmetrically substituted tetraphenylporphyrins[14] and natural porphyrin derivatives[15] was previously reported. The results herein indicate that the introduction of only two alkyl substituents at the β-pyrrole positions of porphine can also produce significant changes in the spin density of the resulting iron(III) complexes to be detected by ^{1}H NMR spectroscopy.

The ground electronic state of low-spin iron(III) porphyrins evolves between two extreme cases, i.e. $(d_{xy})^2(d_{xz},d_{yz})^3$ and $(d_{xz}d_{yz})^4(d_{xy})^1$[9] The ^{1}H NMR spectra of the bis(cyanido) complexes of many artificial iron(III) porphyrins[16] and some naturally derived ferriheme[15] complexes were reported. The former studies generally indicated that the electronic ground state was $(d_{xy})^2(d_{xz},d_{yz})^3$ for these complexes. However, more recently, it was shown that the bis(cyanido) complexes of *meso*-substituted Fe^{III} porphyrins having alkyl substituents of increasing size[17] and other iron(III) porphyrins having bulky substituents in the *meso* position[18–21] show a large shift in the pyrrole protons towards the diamagnetic region, which is indicative of a large contribution of the unusual $(d_{xz}d_{yz})^4(d_{xy})^1$ electronic configuration to the ground state. Furthermore, this situation is amplified when the NMR spectroscopic solvent is methanol because of a possible hydrogen bond between the axial ligand and the solvent.[6,13,22]

^{1}H NMR spectroscopic resonances for the β-pyrrole protons in K[**1**·Fe(CN)$_2$] and K[**2**·Fe(CN)$_2$] appear at very high magnetic field (δ = –10 to –20 ppm). This large upfield shift of the β-pyrrole protons indicates the existence of large spin densities on the β-pyrrole carbons, which is induced by the interactions between porphyrin $3e_g$ and iron d_π orbitals. Because the $3e_g$ orbital places large electron densities on the β-pyrrole carbons, the spin transfer from porphyrin $3e_g$ to iron d_π results in the large spin densities to these carbons, which would be translated as a large upfield shift of the β-pyrrole protons. This is a typical observation for a $(d_{xy})^2(d_{xz},d_{yz})^3$ electronic ground state.[10] By comparison with bis(cyanido)iron porphine,[23] (pyrrole –13.8 ppm, *meso* 1.8 ppm) it should be also noted that a large difference in the spin distribution of the pyrrole in K[**1**·Fe(CN)$_2$] is generated by adding only one methyl group and one ethyl group. In this particular case, all six β-pyrrole protons are detected separately, whereas a single peak at –13.8 ppm is observed for bis(cyanido)iron porphine.[23] It should also be noted that, generally, the ^{1}H NMR spectra of dicyanohemin complexes are well-resolved, as the lines are quite narrow due to very rapid electron spin relaxation times and long proton relaxation times, T_1 and T_2, respectively.[9,24,25] This remarkable resolution was also detected with iron(III) geoporphyrins.[26]

It should be emphasized that the *meso* ^{13}C chemical shift is also particularly useful to determine the electronic configuration.[27,28] Thus, the *meso* carbon signal in complexes with the $(d_{xy})^2(d_{xz},d_{yz})^3$ configuration appears more upfield than the corresponding signal in diamagnetic complexes because the $3e_g$ orbital, which interacts with the half-occupied d_π orbital has a node at the *meso* carbon atom. By contrast, the complexes with a $(d_{xz},d_{yz})^4(d_{xy})^1$ ground state have large spin density at the *meso* carbon as a result of the a_{2u}–d_{xy} interaction, exhibiting a *meso* carbon signal at a downfield position. Thus, it is quite obvious that the values summarized in Table 3 agree well with the $(d_{xy})^2(d_{xz},d_{yz})^3$ configuration and confirm the ^{1}H NMR spectroscopic interpretation.

Conclusions

^{1}H and ^{13}C NMR spectroscopic analysis of β-alkyl-substituted iron porphyrins can be a very sensitive tool to probe the fine details of the electronic structure. This may be relevant to our protein studies with artificial hemes. Analysis of the pyrrole proton and *meso* carbon chemical shifts of K[**1**·Fe(CN)$_2$], K[**2**·Fe(CN)$_2$], and K[**3**·Fe(CN)$_2$] reveals that all complexes show mainly a low-spin $(d_{xy})^2(d_{xz},d_{yz})^3$ electronic ground state.

Thus, the spectroscopic observations are indicative of a metal-based electron in the d_π orbitals of the iron(III) bis(cyano) complexes at any temperature. The change in ground state of low-spin Fe^{III} from the usual

$(d_{xy})^2(d_{xz},>d_{yz})^3$ to the unusual $(d_{xz}d_{yz})^4(d_{xy})^1$ electronic configuration, which was previously suggested to occur from weak hydrogen bonding to the cyanido ligand in methanol solution with *ortho*-substituted tetraphenylporphyrins and even more with highly ruffled porphyrins,[21] is not observed with these *meso*-unsubstituted porphyrins that bear few substituents on the β-pyrrole positions. Accordingly, these results demonstrate the high energy barrier to ruffling, which seems to prevent ring deformation and, consequently, the interaction of the d_{xy} orbital with the $a_{2u}(\pi)$ porphyrin orbital.

Experimental Section

General: All reactions were performed under an atmosphere of argon. Solvents were distilled from appropriate drying agent prior to use: Et_2O and THF from sodium and benzophenone, toluene from sodium, CH_2Cl_2 from CaH_2, $CHCl_3$ from P_2O_5, and all other solvents were HPLC grade. Commercially available reagents were used without further purification unless otherwise stated. All reactions were monitored by TLC with Merck precoated aluminium foil sheets (Silica gel 60 with fluorescent indicator UV_{254}). Compounds were visualized with UV light at 254 and 365 nm. Column chromatography was carried out by using silica gel from Merck (0.063–0.200 mm). High-resolution mass spectra were recorded with a ZabSpec TOF Micromass spectrometer in ESI positive mode at the CRMPO. Liquid UV/Vis spectra were recorded with a UVIKON XL from Biotech. ^{1}H and ^{13}C NMR in $CDCl_3$ were recorded with a Bruker Avance 500 operating at 500.15 MHz for ^{1}H and 125.769 MHz for ^{13}C with a 5 mm broadband probe equipped with a *z*-gradient coil. The spectral widths were adjusted depending on the spin state of the compounds, with 200 and 45 ppm for the proton spectra of high-spin and low-spin complexes, respectively. The ^{13}C spectral width was 400 ppm for the low-spin complexes. Standard Bruker pulse programs were used for the acquisition of the 2D COSY, HSQC, and HMBC[29,30] spectra. Because of the paramagnetism of the derivatives, relatively short relaxation rates (R_1 and R_2) are expected. Consequently, recycling times of 0.5 and 0.8 s were used for the high-spin and the low-spin complexes. For the heteronuclear experiments, despite the large spectral width in the ^{13}C dimension spectra, 2 K × 256 points were recorded. Some spectra were recorded with a Bruker Avance 300. The syntheses of β-pyrrole-substituted porphyrins **1**, **2**, and **3** were previously reported.[4,31]

Preparation of Iron Porphyrins

1·Fe^{III}Cl: Iron was inserted following the procedure of Borovkov et al.[32] 3-Ethyl-2-methylporphyrin **1** (190 mg, 0.51 mmol) was dissolved in distilled chloroform (75 mL). $FeCl_2{\cdot}4H_2O$ (16 equiv.) dissolved in distilled methanol (50 mL) and two drops of 2,6-lutidine were then added. The reaction mixture was stirred at 50 °C and monitored by thin-layer chromatography (TLC) until completion. After evaporation of the solvent, the crude product was purified by column chromatography (CH_2Cl_2/MeOH, 3%). Before total evaporation, two drops of concentrated hydrochloric acid were added. Recrystallization from dichloromethane/pentane afforded 3-ethyl-2-methylporphyrin iron chloride **1·FeCl** as a black powder (100 mg, 0.24 mmol, 40%). ^{1}H NMR (500 MHz, $CDCl_3$, 298 K): δ = –63.3 (s, 2 H, *meso*-H), –58.3 (s, 2 H, *meso*-H), 39.9 and 43.7 (s, 2 H, CH_2CH_3), 51.3 (s, 3 H, CH_3), 76.8, 77.7, and 78.6 (6 H, pyrrol-H) ppm. UV/Vis: λ (ε, mM^{-1} cm^{-1}) = 371 (110), 496 (10), 522 (10.7), 564 (3.2), 623 (5.8) nm. HRMS (LSIMS-MS): calcd. for $C_{23}H_{18}{}^{35}Cl^{56}FeN_4$ $[M]^{+\cdot}$ 441.0569; found 441.0574.

2·FeCl: Prepared as per **1·FeCl**. Yield: 75%. ^{1}H NMR (500 MHz, $CDCl_3$, 298 K): δ = –63.3 (s, 1 H, α/γ-H), –59.3 (s, 2 H, β,δ-H), –53.8 (s, 1 H, α/γ-H), 40.4 and 43.3 (s, 4 H, CH_2CH_3), 54.0 (s, 6 H, CH_3), 76.8 and 79.06 (s, 4 H, pyrrol-H) ppm. UV/Vis (CH_2Cl_2): λ (ε, mM^{-1} cm^{-1}) = 375 (114.6), 499 (12.4), 525 (10.7), 570 (3.8), 627 (5.8) nm. HRMS (ESI-MS): calcd. for $C_{26}H_{24}{}^{56}FeN_4$ $[M – Cl]^+$ 448.1350; found 448.1355.

3·FeCl: Prepared as per **1·FeCl**. Yield: 55%. ^{1}H NMR (500 MHz, $CDCl_3$, 298 K): δ = –56.6 (s, 2 H, *meso*-H), –54.9 (s, 2 H, *meso*-H), 40.5 and 43.9 (s, 8 H, CH_2CH_3), 52.5 (s, 12 H, CH_3) ppm. UV/Vis (CH_2Cl_2): λ (ε, mM^{-1} cm^{-1}) = 379 (98.9), 505 (8.4), 534 (8.5), 635 (4.4) nm. HRMS (ESI-MS): calcd. for $C_{32}H_{36}{}^{56}FeN_4$ $[M – Cl]^+$ 532.2289; found 532.2292.

Preparation of the Dicyanido-Ligated Complexes: Usually, these complexes were prepared in situ by dissolution of 2–3 mg of the respective high-spin complex in [D_1]chloroform/[D_4]MeOH solution (60:40) saturated with KCN. Under these experimental conditions, the black solution turned red, which is characteristic of the formation of the low-spin dicyano complex.

K[1·Fe(CN)$_2$]: ^{1}H NMR (500 MHz; $CDCl_3$/MeOD, 60:40; 298 K): δ = –15.32 (s, 1 H, 8-H), –14.93 (s, 1 H, 17-H), –13.59 (s, 1 H, 12/13-H), –13.49 (s, 1 H, 12/13-H), –12.38 (s, 1 H, 18-H), –12.25 (s, 1 H, 7-H), 0.07 (s, 1 H, β/γ-H), 0.12 (s, 1 H, β/γ-H), 0.68 (t, J = 5 Hz, 3 H, CH_2CH_3), 2.38 (s, 1 H, δ-H), 2.77 (s, 1 H, α-H), 8.62 (q, J = 5 Hz, 2 H, CH_2CH_3), 18.89 (s, 3 H, CH_3) ppm. ^{13}C NMR (125 MHz; $CDCl_3$/MeOD, 60:40): δ = –39.99 (CH_3), –27.10 (CH_2CH_3), 51.42 (C-α), 53.81 (C-δ), 72.14 (C-7), 74.14 (C-18), 83.10 (C-β), 83.30 (C-γ), 86.89 (CH_2CH_3), 94.66 (C-12/13), 94.86 (C-12/13), 102.04 (C-17), 104.03 (C-8) ppm.

K[2·Fe(CN)$_2$]: ^{1}H NMR (500 MHz; $CDCl_3$/MeOD, 60:40; 298 K): δ = –14.43 (s, 2 H, 13,17-H), –11.48 (s, 2 H, 12,18-H), –0.98 (s, 1 H, γ-H), 0.50 (t, J = 5 Hz, 6 H, CH_2CH_3), 1.29 (s, 2 H, β,δ-H), 3.72 (s, 1 H, α-H), 7.02 (q, J = 5 Hz, 4 H, CH_2CH_3), 18.87 (s, 6 H, CH_3) ppm. ^{13}C NMR (125 MHz; $CDCl_3$/MeOD, 60:40): δ = –42.2 (CH_3), –22.7 (CH_3CH_2), 28.3 (C-1,9), 32.19 (C-11,19), 35.83 (C-α), 62.14 (C-4,6), 62.96 (C-14,16), 65.4 (C-β,δ), 76.18 (C-12,18), 77.8 (CH_2CH_3), 97.26 (C-γ), 107.5 (C-13,17), 107.62 (C-3,7), 142.1 (C-2,8) ppm.

K[3·Fe(CN)$_2$]: ^{1}H NMR (500 MHz; $CDCl_3$/MeOH, 60:40; 298 K): δ = 0.44 (t, J = 5 Hz, 12 H, CH_2CH_3), 1.43 (s, 2 H, β,δ-H), 2.18 (s, 2 H, α,γ-H), 7.30 (q, J = 5 Hz, 8 H, CH_2CH_3), 16.71 (s, 12 H, CH_3) ppm. ^{13}C NMR (125 MHz; $CDCl_3$/MeOH, 60:40): δ = –37.46 (CH_3), –22.54 (CH_2CH_3), 39.85 (C-1,9,11,19), 47.22 (C-4,6,14,16), 57.06 (C-α,γ), 60.34 (C-β,δ), 77.72 (CH_2CH_3), 127.38 (C-2,8,12,18), 131.80 (C-3,7,13,17) ppm.

[1] Y. Lu, S. M. Berry, T. D. Pfister, *Chem. Rev.* **2001**, *101*, 3047–3080.
[2] T. Hayashi, Y. Hisaeda, *Acc. Chem. Res.* **2002**, *35*, 35–43.
[3] S. Neya, N. Fiunasaki, T. Sato, N. Igarashi, N. Tanaka, *J. Biol. Chem.* **1993**, *268*, 8935–8942.
[4] S. Juillard, G. Simonneaux, *Synlett* **2006**, *17*, 2818–2820.
[5] S. Juillard, A. Bondon, G. Simonneaux, *J. Inorg. Biochem.* **2006**, *100*, 1441–1448.
[6] G. N. La Mar, J. Del Gaudio, J. S. Frye, *Biochim. Biophys. Acta* **1977**, *498*, 422–435.
[7] I. Morishima, S. Kitagawa, E. Matsuki, T. Inubushi, *J. Am. Chem. Soc.* **1980**, *102*, 2429–2437.
[8] H. Kalish, J. E. Camp, M. Stepien, L. Latos-Grazynski, M. M. Olmstead, A. L. Balch, *Inorg. Chem.* **2002**, *41*, 989–997.

[9] F. A.Walker, "Proton NMR and EPR Spectroscopy of Paramagnetic Metalloporphyrins" in *The Porphyrin Handbook* (Eds.: K. M. Kadish, K. M. Smith, R. Guilard), Academic Press, San Diego, CA, **2000**, vol. 5, ch. 36, pp. 81–183.
[10] G. N. La Mar, F. A. Walker, *The Porphyrins* (Ed.: D. Dolphin), Academic Press, New York, **1979**, vol. 4, pp. 61–157.
[11] J. Wojaczynski, L. Latos-Grazynski, W. Hrycyk, E. Pacholska, K. Rachlewicz, L. Szterenberg, *Inorg. Chem.* **1996**, *35*, 6861–6872.
[12] M. Nakamura, *Coord. Chem. Rev.* **2006**, *250*, 2271–2294.
[13] A. Ikezaki, M. Nakamura, *Inorg. Chem.* **2002**, *41*, 2761–2768.
[14] H. Tan, U. Simonis, N. Shokhirev, F. A. Walker, *J. Am. Chem. Soc.* **1994**, *116*, 5784–5790.
[15] G. N. La Mar, D. B. Viscio, K. M. Smith, W. S. Caughey, M. L. Smith, *J. Am. Chem. Soc.* **1978**, *100*, 8085–8092.
[16] F. A. Walker, *Coord. Chem. Rev.* **1999**, *185–186*, 471–534.
[17] M. Nakamura, T. Ikeue, H. Fujii, T. Yoshimura, *J. Am. Chem. Soc.* **1997**, *119*, 6284–6291.
[18] S. Wolowiec, L. Latos-Grazynski, M. Mazzanti, J. C. Marchon, *Inorg. Chem.* **1997**, *36*, 5761–5771.
[19] J. Wojaczynski, L. Latos-Grazynski, T. Glowiak, *Inorg. Chem.* **1997**, *36*, 6299–6306.
[20] S. Wolowiec, L. Latos-Grazynski, M. Mazzanti, J. C. Marchon, *Inorg. Chem.* **1998**, *37*, 724–732.
[21] M. Nakamura, T. Ikeue, A. Ikezaki, Y. Ohgo, H. Fujii, *Inorg. Chem.* **1999**, *38*, 3857–3862.
[22] G. Simonneaux, F. Hindré, M. Le Plouzennec, *Inorg. Chem.* **1989**, *28*, 823–825.
[23] K. Wüthrich, *Struct. Bonding (Berlin)* **1970**, *8*, 53–121.
[24] S. W. Unger, T. Jue, G. N. La Mar, *J. Magn. Reson.* **1985**, *61*, 448–456.
[25] I. Bertini, P. Turano, A. Vila, *J. Chem. Rev.* **1993**, *93*, 2833–2932.
[26] S. Wolowiec, L. Latos-Grazynski, O. Serebrennikova, F. Czechowski, *Magn. Reson. Chem.* **1995**, *33*, 34–43.
[27] T. Ikeue, Y. Ohgo, T. Saitoh, M. Nakamura, H. Fujii, M. Yokoyama, *J. Am. Chem. Soc.* **2000**, *122*, 4068–4076.
[28] T. Ikeue, Y. Ohgo, T. Saitoh, T. Yamaguchi, M. Nakamura, *Inorg. Chem.* **2001**, *40*, 3423–3434.
[29] M. F. Summers, L. G. Marzilli, A. Bax, *J. Am. Chem. Soc.* **1986**, *108*, 4285–4294.
[30] A. Bax, D. Marion, *J. Magn. Reson.* **1988**, *78*, 186–191.
[31] S. Juillard, Y. Ferrand, G. Simonneaux, L. Toupet, *Tetrahedron* **2005**, *61*, 3489–3495.
[32] V. V. Borovkov, J. M. Lintuluoto, Y. Inoue, *Synlett* **1999**, *1*, 61–62.
[33] D. V. Behere, R. Birdy, S. Mitra, *Inorg. Chem.* **1982**, *21*, 386–390.

Received: May 9, 2007
Published Online: July 12, 2007

